

# The Effect of Process Parameters and Tool Geometrical Parameters on the Tool Peak Temperature in Machining Process

**Maziar Mahdipour Jalilian\***

Department of Mechanical Engineering,  
Kermanshah Branch, Islamic Azad University, Kermanshah, Iran  
E-mail: Maziar.1986.2000@gmail.com

\*Corresponding author

**Amir Ghiasvand**

Department of Mechanical Engineering,  
University of Tabriz, Iran  
E-mail: Amir.Ghiasvand@Tabrizu.ac.ir

**Hasan Kheradmandan**

Department of Mechanical Engineering,  
Kermanshah Branch, Islamic Azad University, Arak, Iran  
E-mail: Kheradmandan.hasan@gmail.com

**Received: 13 November 2020, Revised: 19 March 2021, Accepted: 25 March 2021**

**Abstract:** In the present study, the effects of process and geometrical parameters on the maximum temperature of tool have been investigated. Simulation of mild steel machining process in different cutting depths, speed of rotation (SOR), feeding rates, and different rake angles was performed. To verify the simulation, numerical results were compared with experimental results. Based on the results, it was found that by increasing the speed of rotation at a constant cutting depth and a constant feed rate, the maximum temperature of the process experiences a significant increase. By increasing the depth of the cut, the geometric location of the workpiece maximum temperature was transmitted to the edge of the tool and surface changes occurred, which it was accompanied with increment in the depth of the cut. The tool with the rake angle of  $-10^\circ$  and the depth of cutting of 2 mm had the highest recorded temperature due to the lack of sufficient space for removing chips from the work surface.

**Keywords:** Geometrical Parameters, Machining, Tool Shape, Tool Temperature

**How to cite this paper:** Maziar Mahdipour Jalilian, Amir Ghiasvand, and Hasan Kheradmandan, "The Effect of Process Parameters and Tool Geometrical Parameters on the Tool Peak Temperature in Machining Process", Int J of Advanced Design and Manufacturing Technology, Vol. 14/No. 3, 2021, pp. 75–83.  
DOI: 10.30495/admt.2021.1914924.1228

**Biographical notes:** **Maziar Mahdipour Jalilian** is assistant professor in the Department of Mechanical Engineering, Engineering Faculty, Islamic Azad University of Kermanshah, Kermanshah, Iran. He obtained his PhD degree from Razi University in 2017. His working field includes various welding and machinery equipment simulation, composite structures and nano-materials. **Amir Ghiasvand** received his PhD Graduated from Tabriz University in 2020. His research interest includes mechanical phenomena numerical simulation, Friction Stir Welding (FSW) and fatigue. He is now searching for a Post-Doc position. **Hasan Kheradmandan** is a PhD student in Arak Azad University. He received his MSc in Mechanical Engineering from Islamic Azad University, Arak Branch, Arak, Iran, in 2017. His research field includes Friction Stir Welding (FSW). He is expanding his experience in numerical simulation.

## 1 INTRODUCTION

High Speed Machining (HSM) is one of important industrial processes which is classified in relatively modern techniques which has higher capability and efficiency in comparison with other machining processes [1]. The advantages of this method include high accuracy and quality of produced parts, precise production of parts, ability of high hardness materials machining and high production efficiency [2-4].

In HSM, a large amount of heat is generated in tool and its contact area with workpiece which is because of two main factors: small contact area [5] and forming relatively adiabatic situation due to high speed machining and lack of fast and proper heat transfer to other parts [4]. Due to two mentioned parameters, generated heat is trapped in a small area and significant temperature increment occurs. In addition to generated heat, other parameters like contact between workpiece and detached chips, tool feed rate, tool cutting speed, cut depth and tool geometry affect the temperature increment. A change in each mentioned parameters, results in change in generated heat amount and consequently the maximum temperature of process [6]. Because of high speed and accumulated heat at tip of tool, corrosion and erosion usually take place at tool tip [7-8]. Tool geometry has a direct effect on heat generation and shear force amount. Tool has two main angles named rake angle and flank angle [2], [5]. By changing each angle, noticeable change occurs in process temperature and exerted force on tool [9].

Relatively large number of researches have been performed in temperature distribution in machining which usually have focused on workpiece temperature conditions and distribution [10-13]. A few researches have been done on geometrical parameters effects on generated heat and temperature distribution. Therefore, there is a need for more research in this area. Therefore, in the present study, the effect of process parameters and geometric parameters of the tool on the temperature distribution and maximum temperature of the tool has been investigated. Numerical simulation was performed using Arbitrary Lagrangian-Eulerian (ALE) method by ABAQUS software. Numerical simulation verification was done using experimental results. After that, the effects of process parameters and geometric parameters of the tool on heat generation and the maximum temperature were investigated.

## 2 EXPERIMENTS

To verify the numerical results, experimental ones have been used. In order to check the accuracy of numerical models, numerical results have been compared with experimental ones. For this purpose, the machining process was performed with a tool with specific geometric parameters at different rotational speeds.

Using temperature data obtained from experimental work and comparing these results with numerical results, the accuracy of numerical models was investigated. In the experimental work, a tool was used which its tip and shank were made of WC high carbon steel and cast iron, respectively. The workpiece used in the experimental work was made of mild steel. The workpiece was prepared as a shaft with diameter of 20 mm and length of 200 mm.

The tool used in the experimental work had a rake angle of 20 degrees and a flank angle of 5 degrees. In the experimental work, the machining process was performed at a cutting depth of 1 mm and a feed rate of 3 cm/min. The rotational speed of the workpiece was considered in 5 different states and the peak temperature of the tool was recorded for each of the states. In order to record the peak temperature of the tool during the machining process, an infrared thermometer was used which is shown in "Fig. 1".



Fig. 1 Used infrared thermometer.

The thermometer was connected to a recording device so that the temperature at every machining step could be recorded at different rotational speeds. Figure 2 shows how to install a thermometer and record the temperature.



Fig. 2 Recording temperature during machining.

### 3 NUMERICAL SIMULATION

Due to the costs and complexities of machining process experiments and the impossibility of performing experiments for all cases with different speeds and depths of cuts, numerical simulation of machining process has always been of interest to researchers and is of great importance [14]. With correct numerical simulation and according to the nature of the process, it is possible to make a good prediction of the temperature distribution, forces on the tool, stress and strain patterns in the tool and the workpiece. It should be mentioned that the machining process is vertical. This process can be modeled in two dimensions because the heat distribution and stress patterns in the tool are created in a small two-dimensional surface and the changes of these factors in the thickness direction are small. This two-dimensional assumption makes the numerical simulation of the process more flexible. Due to the presence of plastic displacements and large plastic strains, as well as surface chipping of the workpiece, appropriate technic should be used to model the process to bring the simulation conditions of the problem closer to the real conditions. Due to the fact that Lagrangian modeling of the machining process causes limitations in applying large deformations to the elements, an alternative and efficient technique should be used for numerical simulation of the machining process [15]. In the current study, the ALE modeling technique has been used to numerically simulate the machining process. In this manner, the part of the workpiece that is in contact with the tool and faces large plastic strains is simulated using ALE technique. The ALE elements have a higher ability to deform and also the problem of deviation in these elements and of course the failure of the analysis are eliminated. The following steps are required to numerically simulate the process.

#### 3.1. Geometric Modeling, Material Properties

The tool and the workpiece were both modelled deformable and two-dimensional. The dimensions of the workpiece according to the maximum cutting depth were considered in such a way that heat transfer to the workpiece was considered appropriate. The length of the workpiece was 20 times and its width was 6 times the maximum cutting depth in experimental conditions. Thus According to the experimental conditions, the workpiece in the initial stage of the simulation was considered to be 40 mm length and 6 mm width. Also, in the first stages of numerical simulation (steps performed to verify the numerical models) Flank and rake angles were considered equal to 5 and 20 degrees, respectively.

Due to the thermomechanical nature of the machining process, in addition to defining the mechanical properties of the parts, it is necessary to define the thermal properties of the tool and workpiece in the numerical simulation process. In all studied cases,

according to the experimental conditions, the tool tip, shank and the workpiece were made of high carbon steel (WC), cast iron and mild steel, respectively. The mechanical and thermal properties of the tool and the workpiece have been presented in “Table 1” . According to the heat generation factors in the process, it was assumed that 90% of the energy generated by the plastic deformation of the workpiece is converted to heat. Therefore, in the definition of the workpiece material inelastic heat loss parameter was considered as 0.9.

**Table 1** Mechanical properties of tool and workpiece [16]

Properties	Mild Steel	Cast Iron	High Carbon Steel
$\rho(\text{Kg/m}^3)$	7850	7200	1500
E(GPa)	207	120	800
$\nu$	0.2	0.26	0.2
C(J/Kg.C)	477	450	200
K(W/m.c)	44	46	46
$\alpha(10^{-6}/\text{C})$	1.3	0.11	4.7

In order to model the machining conditions and plastic strains in the part, the Johnson-Cook model was used. In this model, the stress is considered as a function of strain, strain rate and temperature. The amount of yield stress at each moment of the process is calculated with a high accuracy.

$$\sigma = \left( A + B\varepsilon^n \right) \left[ 1 + C \ln \frac{\dot{\varepsilon}}{\dot{\varepsilon}_0} \right] \left[ 1 - \left( \frac{T - T_r}{T_m - T_r} \right)^m \right] \quad (1)$$

In this Equation,  $\sigma$  is the yield stress at any moment of the process and A, B, C, n and m are the material constants.  $T$ ,  $T_r$  and  $T_m$  are the instantaneous temperature, transfer temperature and the melting temperature of the material, respectively [17]. By knowing the above parameters, the stress and strain in the plastic phase of the material can be calculated correctly.

Due to the nature of the machining process and the existence of phase and mechanical damage step in the part, the appropriate damage conditions should be defined and attributed to the part in order to be able to model the chip removal from the part surface. For this purpose, Johnson-Cook's damage Equation has been used to predict the onset of damage step and its development. The relations are presented in Equations (2) and (3) [18].

$$D = \sum \left( \frac{\Delta\varepsilon^{-pl}}{\varepsilon_f^{-pl}} \right) \quad (2)$$

$$\varepsilon_f^{-pl} = \left[ d_1 + d_2 \exp \left( d_3 \frac{\sigma_p}{\sigma_e} \right) \right] \left[ 1 + d_4 \ln \left( \frac{\dot{\varepsilon}^{pl}}{\dot{\varepsilon}_0} \right) \right] \left[ 1 - d_5 \left( \frac{T - T_r}{T_m - T_r} \right)^m \right] \quad (3)$$

In this criterion, the removal of the element occurs when the considered plastic strain rate  $\bar{\epsilon}^{pl}$  is equal to failure plastic strain  $\bar{\epsilon}_f^{pl}$ . In this situation, the parameter  $D$  of material is equal to one, which leads to the removal of the desired element during analysis. At this moment the damage condition is met. In order to calculate the plastic strain at the failure moment of, Equation (3) was used. In this Equation,  $d_1 - d_5$  are the material damage constants obtained by Hopkinson test.  $\sigma_p$  and  $\sigma_e$  are hydrostatic stress and von Mises stress, respectively. To calculate the damage evolution, the displacement criterion at the moment of failure was used. "Table 2" shows the constants of plastic Equations and Johnson-Cook mild steel damage for two Equations (1) and (3), respectively [19]. Considering the non-forming of the tool and the lack of plastic flow in it, this part was considered to be completely elastic and no plastic properties were used for the tool and only its elastic and thermal properties were considered.

**Table 2** Johnson-Cook constants for mild steel [16]

A(MPa)	B(MPa)	C	n	m
217	233.17	0.0134	0.255	1.078
D1	d2	d3	d4	d5
0.25	4.38	-2.68	0.002	0.61

### 3.2. Model Assembly and Problem-Solving Steps

In order to assemble the numerical model, the position of the tool relative to the workpiece shoulder was set based on the cutting depth in each mode of the simulation. The solution was considered as a temperature-displacement coupled one and Abaqus Explicit solver was used for this purpose. The time in each step was calculated based on the cutting speed. The cutting speed in each position of the simulation was calculated based on the initial diameter of the experimental sample using Equation (4).

$$V_c = \frac{\pi d N}{60} \quad (4)$$

In this Equation,  $N$  and  $d$  are the rotational speed and the initial diameter of the workpiece, respectively. According to the experimental conditions and 20 mm diameter of the workpiece, based on the speed obtained in each simulation mode and the length of 40 mm of workpiece, the time interval of each problem solving-step in each step was calculated and defined.

### 3.3. Loading, Mesh, and Interaction

In order to model the frictional conditions, the Coulumb friction model was used, which its Equation is as follows [20].

$$\begin{aligned} \mu \sigma_n \geq \tau_{\max} &\rightarrow \tau_f = \tau_{\max} \\ \mu \sigma_n < \tau_{\max} &\rightarrow \tau_f = \mu \sigma_n \\ \tau_{\max} &= \frac{\sigma_y}{\sqrt{3}} \end{aligned} \quad (5)$$

In this Equation,  $\tau_f$  is the shear stress due to friction. This shear stress is considered as a specified conditional condition. In order to determine the  $\tau_{\max}$ , Von-Mises criterion was used that is equal to the specified Equation, in which  $\sigma_y$  is the yield stress of the workpiece. The value of the friction coefficient in the developed Coulumb relation was considered as 0.6. Due to the thermal deliberation of the tool and the assuming no initial plastic strain and its creation of plastic strain in the tool, rigid body constraint was used. The upper corner of tool was considered as reference point and all degrees of freedom were set constraint.

Also, due to the temperature-displacement coupling of the problem, elements containing degree of thermal freedom were used. During the modeling of the samples, the workpiece was divided into two separate sections and each of these two sections was assigned a specific grain size. Finally, after analyzing the sensitivity of the mesh and using meshes with different grain sizes, the workpiece and tool were meshed with 9860 and 186 elements from CPE4RT family, respectively, ("Fig. 3").

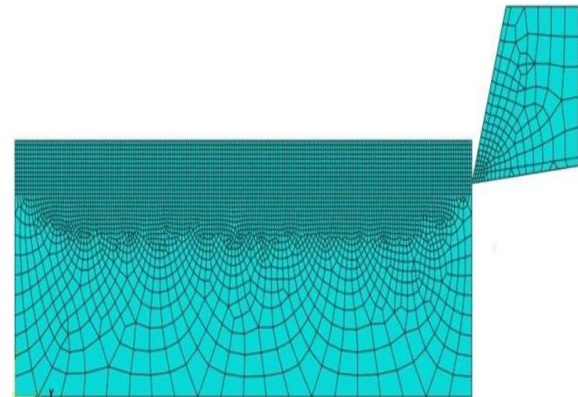


**Fig. 3** Used infrared thermometer.

## 4 RESULTS AND DISCUSSION

In order to verify the simulation, the results of the maximum temperature in the instrument in several experimental modes with different rotational speeds of workpiece were compared with the numerical solution results. Figure 4 shows a comparison of numerical and experimental results of the maximum temperature at the tip of the tool at a cutting depth of 1 mm and a feed rate of 3 cm / min at different rotational speeds.

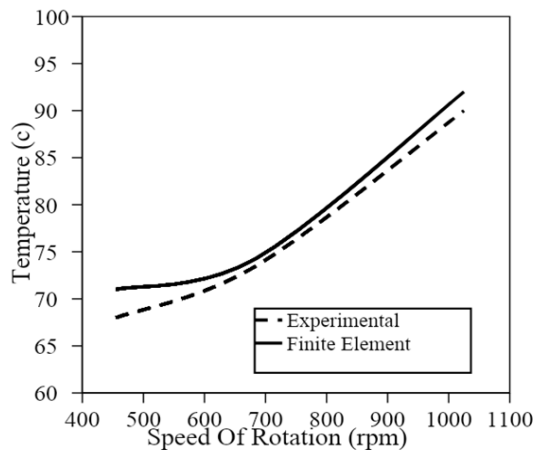


Fig. 4 Comparison between experimental and numerical results.

According to “Fig. 4”, the numerical results are in good agreement with experimental data which confirm the accuracy of numerical simulation conditions and the results obtained in the continue of the paper. In order to model the frictional conditions, the Columb friction model was used, which its Equation is as follows [20].

**4.1. The Effects of Process Parameters**

Figure 5 shows the temperature distribution contour in the tool and workpiece at different rotational speeds (cutting depth 1 mm and feed rate 3 cm/min).

According to “Fig. 5”, it was found that by increasing the rotational speed of the workpiece at a constant feed rate and depth of cut, the maximum temperature in the tool and the chips created increase due to the higher contact rate of the tool and the workpiece. The tool covers a larger surface at shorter time and therefore the contact of the tool tip with the surface of the workpiece increases and higher friction occurs in this area. So, the temperature increases significantly in a short time compared to other surfaces involved in the tool. It should be noted that according to the results of conducted researches, by increasing the rotational speed of the workpiece, the amount of contact stresses on the tool increases, which ultimately leads to increasing the erosion and surface corrosion of the tool and reduces its life [12]. According to the contour of “Fig. 5”, it was found that by changing the rotational speed of the workpiece at constant cutting depth and feeding rate, the temperature distribution and maximum temperature in the workpiece do not experience significant changes and temperature increase occurs at different surfaces of the workpiece which indicates the low effect of changing the rotational speed of the part on the maximum temperature and temperature distribution in the part.

In the following, the effect of other process parameters (feed rate and cutting depth) on the distribution and maximum temperature in the tool has been investigated. Figure 6 shows the temperature changes of the tool and

workpiece at a constant rotational speed (445 rpm) and cutting depth of 0.5 mm for different feed rate values.

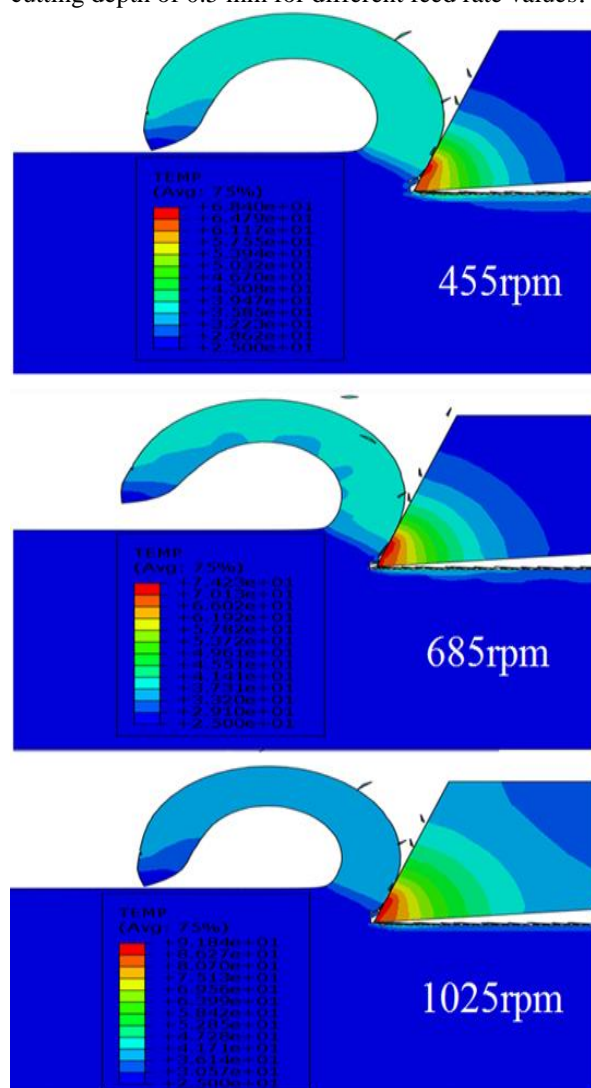


Fig. 5 Contour of temperature at different rotational speeds.

It was found that by increasing the feed rate, the tool has a shorter time to cut a certain surface, and this causes the surface involved in frictional contact and plastic displacements to reduce partly, and of course by reducing these two factors which are the main sources of heat generation in the process, the amount of heat generated in the tool and the part reduces. It should be noted that by increasing the feed rate, the rate of heat transfers from the tip of the tool to its shank decreases and the temperature in a smaller area in the tool increases sharply. Changing the cutting depth of the piece can greatly affect the amount of heat generated in the process. By increasing the cutting depth at constant rotational speed and feed rate, a larger surface of the tool collides with the not deformed surface of the workpiece over a similar period of time, creating greater frictional forces, which increases the plastic strain generation and the maximum temperature in the workpiece and tool.

The larger contact surface between the tool and the workpiece leads to the flow of heat generated in a wider area of the tool. This increment in temperature causes increase in thermal stresses and their concentration which if not controlled, will cause the part of the tool that is in contact with the workpiece, meet the damage area. After that corrosion and gradual erosion will occur.

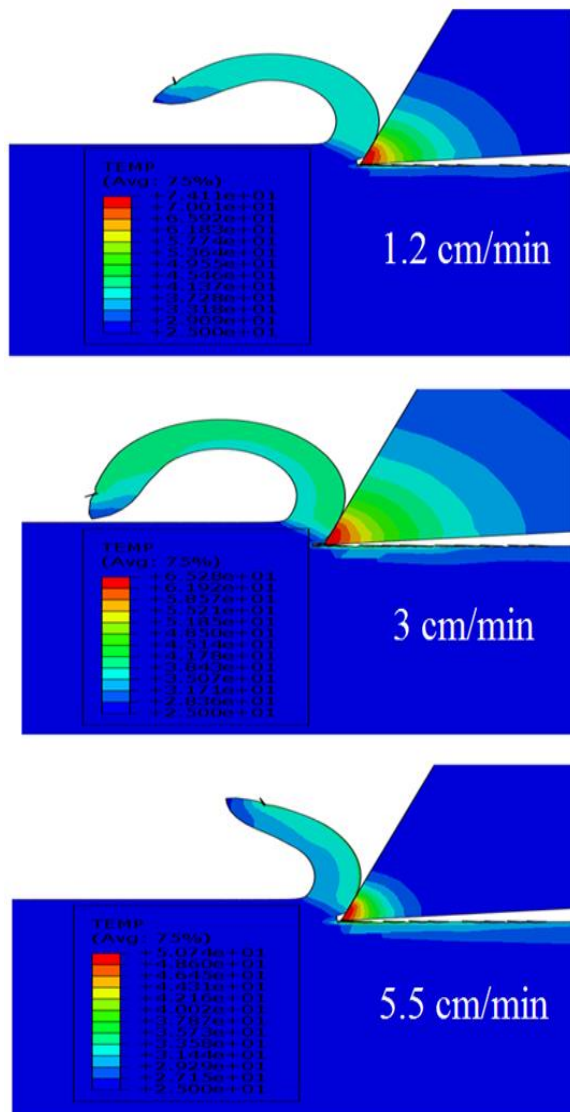


Fig. 6 Contour of temperature for different feed rate values.

Figure 7 shows a diagram of the maximum temperature in the tool based on the simulation results at a constant feed rate of 3 cm / min for different rotational speeds and cutting depths. According to “Fig. 7” and the explanations mentioned in the previous paragraph, it can be seen that by increasing the cutting depth at constant rotational speed and feeding rate, the maximum temperature in the tool increases continuously. It should be noted that in all three rotational speeds, the slope of the maximum temperature vs. cutting depth diagram is relatively zero which again confirms the negligible

effect of the rotational speed parameter of the workpiece on the maximum temperature in the tool.

It is observed that by increasing the cutting depth at constant rotational speed and feeding rate, the maximum temperature in the tool increases continuously. It should be noted that in all three rotational speeds, the slope of the maximum temperature vs. cutting depth diagram is relatively zero which the slope of the temperature increase diagram is relatively equal to the increase in cutting depth, and this again confirms the negligible effect of rotational speed of the workpiece on the maximum temperature in the tool. Another influential parameter on temperature distribution in the machining process is the tool feed rate, which strongly affects the patterns of temperature and stress distribution in the tool and the workpiece during the process.

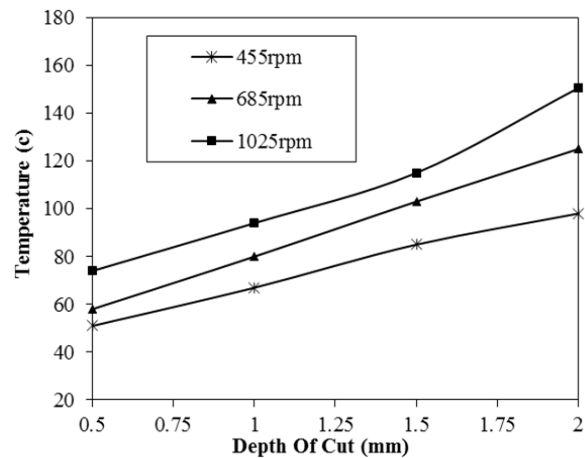


Fig. 7 Tool maximum temperature changes vs. cutting depths.

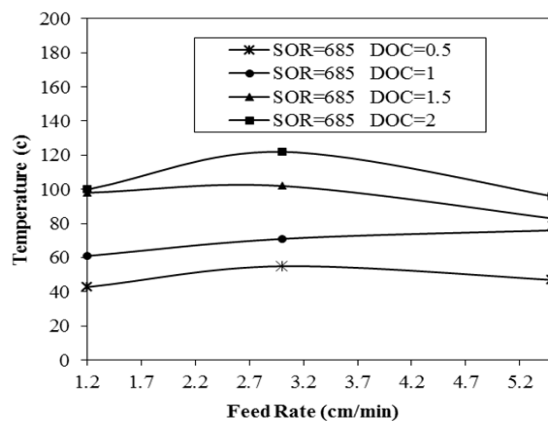


Fig. 8 Maximum tool temperature vs. various feed rates.

Figures 8 and 9 show the diagrams of tool temperature vs. feed rate and cutting depth at constant rotational speeds, which are related to the two rotational speeds of 685 and 1025 rpm, respectively. According to “Figs. 8 and 9”, the increase in feed rate has less effect on larger cutting depths. By increasing the tool feed rate at a constant rotational speed at cutting depths of 1.5 and 2 mm, fewer changes in maximum temperature can be

seen, which is mostly because the contact area value between the tool and workpiece is more dominant than contact time and friction.

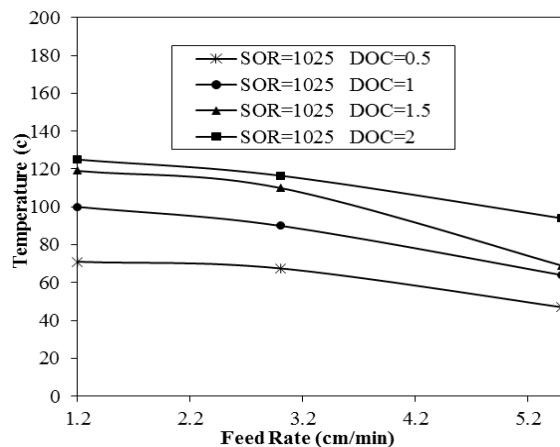


Fig. 9 Maximum tool temperature vs. various feed rates.

### 4.2. Tool Geometry Effect

The effect of rake angle on the maximum temperature of the tool and the temperature distribution in it at four different angles were investigated. These angles were considered to be 10, 0, 20 and -10, respectively. In order to perform a better comparison of results, a constant rotational speed of 1025 and a constant feeding rate of 3 cm / min were used. Figure 10 shows the tool temperature contour with four different rake angles (-10, 0, 10 and 20 ° angles).

According to the presented results, by increasing the rake angle, the temperature of the tool increases sharply, which is due to the increase in the contact area of tool and workpiece. Another noticeable case is the maximum temperature position transfer by changing the rake angle. According to “Fig. 10” and the tool temperature contour, by changing the rake angle value, the maximum temperature position of the tool is transferred from its tip to the cutting edge. It should also be noted that, according to the temperature contour shown in “Fig. 10”, by reducing the rake angle, locus of the maximum temperature covers a wider area at the same time and the maximum temperature location goes to the shank of the tool.

According to “Fig. 10”, in the case of tools with a rake angle of -10 degrees, the highest temperature occurs in the process, which is due to the sharp and continuous increment in the contact surface of the chips with the workpiece and also the lack of suitable exit space for chips removed from the workpiece which leads to the accumulation of heat caused by these chips in the forehead of the tool and causes the temperature of the contact surfaces of the tool and the tool to increase sharply, and finally facilitates and accelerates the gradual erosion and corrosion of the tool.

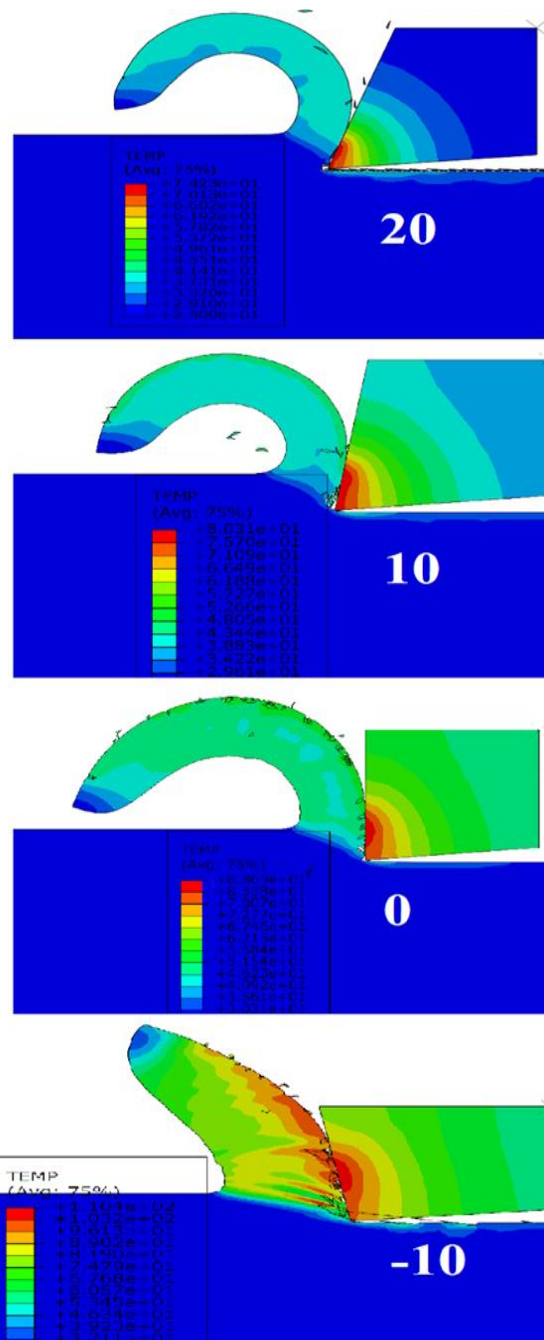
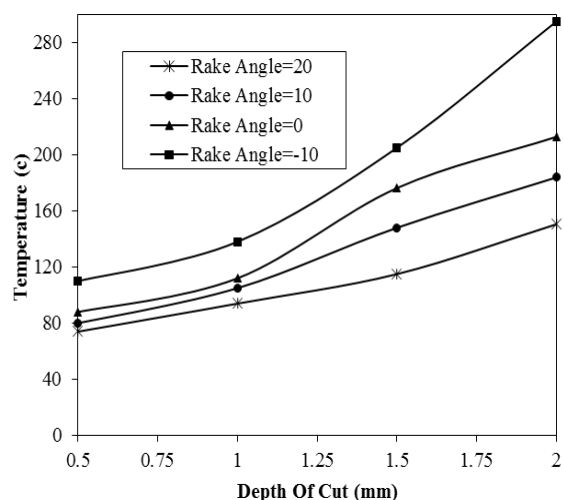


Fig. 10 Tool temperature contour for different rake angles.

Figure 11 shows the results of the simulated maximum temperature changes for different cases of rake angles and cut depths, for feed rate of 3 cm / min and rotational speed of 1025 rpm. According to the diagram, it is clear that in the case of -10° rake angle and maximum cutting depth (2 mm), the highest maximum temperature occurs, which is 1.96 times the maximum temperature in the same case using the tool with the rake angle of 20°. In other words, by changing the rake angle from 20 to -10 degrees, a 96% increase in the maximum temperature in the tool can be seen.

This factor strongly affects the amount of generated thermal stress and strains and the reaction force on the tool and significantly reduces the efficiency, quality of the surfaces and the life of the tool. According to the results of “Fig. 11”, the process of temperature increment occurs more severely with increasing cutting depth and decreasing rake angles, and the tool experiences a higher temperature during this machining course.



**Fig. 11** Changes in maximum temperature at different rake angles.

Use either SI (MKS) or CGS as primary units. (SI units are strongly encouraged.) English units may be used as secondary units (in parentheses). This applies to papers in data storage. For example, write “15 Gb/cm<sup>2</sup> (100 Gb/in<sup>2</sup>).” An exception is when English units are used as identifiers in trade, such as “3½ in disk drive.” Avoid combining SI and CGS units, such as current in amperes and magnetic field in oersteds. This often leads to confusion because Equations do not balance dimensionally. If you must use mixed units, clearly state the units for each quantity in an Equation. The SI unit for magnetic field strength H is A/m. However, if you wish to use units of T, either refers to magnetic flux density B or magnetic field strength symbolized as  $\mu_0 H$ . Use the center dot to separate compound units, e.g., “A·m<sup>2</sup>.”

## 5 CONCLUSION

In present study, the effects of process and geometrical parameters on the maximum temperature of tool have been investigated. Simulation of mild steel machining process in different cutting depths, speed of rotation (SOR), feeding rates and different rake angles was performed using the ALE technique and the ABAQUS 2017 finite element software. The simulation results

were compared with experimental data for verification. The results were as follows:

- 1- Using the ALE technique in machining simulations, the problems caused by large deviations of Lagrangian elements can be overcome, and the analysis fails can be avoided and results can be obtained in close proximity to the experimental results.
- 2- The maximum temperature of the tool at cutting depths of 0.5, 1, 1.5 and 2 mm was investigated and it was found that by increasing the cutting depth at constant rotational speed and feeding rate, a larger maximum temperature occurs in the tool which is due to the increase in the amount of contact area and increase of friction between the tool and the workpiece.
- 3- As the rotational speed of the workpiece increases, a higher amount of heat is generated and consequently a higher temperature occurs in the tool, with higher intensity at greater cutting depths.
- 4- Increasing or decreasing the feed rate had less effect on tool temperature than changing other process parameters. Increasing the feed rate at a constant rotational speed at cutting depths of 1.5 and 2 mm resulted in fewer changes in the maximum temperature due to the predominance of the contact area between the tool and the workpiece over the friction contact time factor between the two surfaces.
- 5- By reducing the rake angle due to the reduction of free space for the removal of chips, this process was performed hardly and therefore the secondary contact of the tool and the chips increased, which led to a sharp increment in the temperature of the tool and workpiece. This increase in temperature happened sharply by decrement in the rake angle.

## ACKNOWLEDGMENTS

This paper is an excerpt from a research project entitled Numerical Simulation of Temperature Distribution in HSM (High Speed Machining) Using ALE Technique, which is funded by Islamic Azad University, Kermanshah Branch.

## REFERENCES

- [1] Hashmi, K. H., Zakria, G., Raza, M. B., and Khalil, S., Optimization of Process Parameters for High Speed Machining of Ti-6Al-4V Using Response Surface Methodology, The International Journal of Advanced Manufacturing Technology, Vol. 85, No. 5-8, 2016, pp. 1847-1856.
- [2] D’addona, S. J. Raykar, and M. Narke, "High speed machining of Inconel 718: tool wear and surface roughness analysis," Procedia CIRP, vol. 62, 2017, pp. 269-274.

- [3] Wang, B., Liu, Z., Evaluation on Fracture Locus of Serrated Chip Generation with Stress Triaxiality in High Speed Machining of Ti6Al4V, *Materials & Design*, Vol. 98, 2016, pp. 68-78.
- [4] Bordin, S., Sartori, S., Bruschi, and Ghiotti, A., Experimental Investigation On the Feasibility of Dry and Cryogenic Machining as Sustainable Strategies When Turning Ti6Al4V Produced by Additive Manufacturing, *Journal of cleaner production*, Vol. 142, 2017, pp. 4142-4151.
- [5] Umbrello, D., Caruso, S., and Imbrogno, S., Finite Element Modelling of Microstructural Changes in Dry and Cryogenic Machining AISI 52100 steel, *Materials Science and Technology*, Vol. 32, No. 11, 2016, pp. 1062-1070.
- [6] T. Özel, T., Zeren, E., Finite Element Modeling the Influence of Edge Roundness On the Stress and Temperature Fields Induced by High-Speed Machining, *The International Journal of Advanced Manufacturing Technology*, Vol. 35, No. 3-4, 2007, pp. 255-267.
- [7] Karpat, Y., Temperature Dependent Flow Softening of Titanium Alloy Ti6Al4V: An Investigation Using Finite Element Simulation of Machining, *Journal of Materials Processing Technology*, Vol. 211, No. 4, 2011, pp. 737-749.
- [8] Ghiasvand, S. Hassanifard, Numerical Simulation of FSW and FSSW with Pinless Tool of AA6061-T6 Al Alloy by CEL Approach, *Journal of Solid and Fluid Mechanics*, Vol. 8, No. 3, 2018, pp. 65-75.
- [9] Cavaliere, P., De Santis, A., Panella, F., and Squillace, A., Effect of Welding Parameters On Mechanical and Microstructural Properties of Dissimilar AA6082-AA2024 Joints Produced by Friction Stir Welding, *Materials & Design*, Vol. 30, No. 3, 2009, pp. 609-616.
- [10] Schmidt, H., Hattel, J., and Wert, J., An Analytical Model for The Heat Generation in Friction Stir Welding, Modelling and Simulation in Materials Science and Engineering, Vol. 12, No. 1, 2003, pp. 143.
- [11] Arrazola, P. J., Investigations on the Effects of Friction Modeling in Finite Element Simulation of Machining, *International Journal of Mechanical Sciences*, Vol. 52, No. 1, 2010, pp. 31-42.
- [12] Marimuthu, P. K., Prasada, T. H., and Kumar, C., 3d Finite Element Model to Predict Machining Induced Residual Stresses Using Arbitrary Lagrangian Eulerian Approach, *Journal of Engineering Science and Technology*, Vol. 13, No. 2, 2018, pp. 309-320.
- [13] F. Jafarian, F., Ciaran, M. I., Umbrello, D., Arrazola, P., Filice, L. and Amirabadi, H., Finite Element Simulation of Machining Inconel 718 Alloy Including Microstructure Changes, *International Journal of Mechanical Sciences*, Vol. 88, 2014, pp. 110-121.
- [14] Akhil M. H., Akhil C K, Afeez, C. K., Akhilesh, P. M., and Rahul Rajan, R., Measurement of Cutting Temperature During Machining, *IOSR Journal of Mechanical and Civil Engineering*, Research Paper, Vol. 13, No. 2, 2016, pp. 108-122.
- [15] Mousavi, S., Kelishami, A. R., Experimental and Numerical Analysis of the Friction Welding Process for the 4340 Steel and Mild Steel Combinations, *Welding Journal New York*, Vol. 87, No. 7, 2008, pp. 178.
- [16] MatWeb, L., MatWeb: Material Property Data, [linea]. Available: <http://www.matweb.com/search/DataSheet.aspx>, 2013.
- [17] Johnson, G. R., Cook, W. H., Fracture Characteristics of Three Metals Subjected to Various Strains, Strain Rates, Temperatures and Pressures, *Engineering fracture mechanics*, Vol. 21, No. 1, 1985, pp. 31-48.
- [18] Duan, C., Dou, T., Cai, Y., and Li, Y., Finite Element Simulation and Experiment of Chip Formation Process During High Speed Machining of AISI 1045 Hardened Steel, *International Journal of Recent Trends in Engineering*, Vol. 1, No. 5, 2009, pp. 46-50.
- [19] Iqbal, M., Senthil, K., Bhargava, P., and Gupta, N., The Characterization and Ballistic Evaluation of Mild Steel, *International Journal of Impact Engineering*, Vol. 78, 2015, pp. 98-113.
- [20] Hibbit, H., Karlsson, B., and Sorensen, E., ABAQUS User Manual, Vol. 6.12, Simulia, Providence, RI, 2012.